This paper was published in International Journal of Rock Mechanics and Mining Sciences, 71, 301-309, doi:10.1016/j.ijrmms.2014.07.001.

Impact of fracture networks on borehole breakout heterogeneities in crystalline rock

David P. Sahara*[1], Martin Schoenball[1], Thomas Kohl[1], Birgit I.R. Müller[1,2]
[1]*Karlsruhe Institute of Technology, Institute of Applied Geosciences, Adenauerring 20b, 76131 Karlsruhe, Germany*
[2]*Landesforschungszentrums Geothermie, Adenauerring 20b, 76131 Karlsruhe, Germany*

david.sahara@kit.edu (D.P.Sahara)

Abstract

Breakouts are commonly used as principal indicator of stress orientation. However, variation of breakout orientation with depth, especially in the vicinity of fracture zones, is frequently observed. This study describes a systematic analysis of breakout occurrence, variation of breakout orientation and fracture characteristics. We infer the impact of fracture networks on the development of breakouts from detailed analysis of 1221 borehole elongation pairs in the vicinity of 1871 natural fractures observed in the crystalline section of the GPK4 well of the Soultz-sous-Forêts geothermal field (France). Breakout orientation anomalies are found to concentrate in the immediate vicinity of fault cores and to decrease with distance to the fault core. Patterns of breakout orientation in the vicinity of natural fractures suggest that the breakout rotation, relative to the mean S_{hmin} direction, is strongly influenced by the fracture orientation. Even a direct relationship between fracture and breakout orientations is found in some depth intervals. In highly fractured zones, with different fracture families present, breakout orientations are especially heterogeneous, resulting from the overlapping effects of the fracture network. Additionally, breakouts are typically found to be asymmetrical in zones with high fracture density. Borehole breakout heterogeneities do not seem to be related to the principal stress heterogeneity only, but also to the effect of mechanical heterogeneities like weak zones with different elastic moduli, rock strength and fracture patterns. Consequently, care has to be taken when inferring the principal stress orientation from borehole breakout data observed in fractured rock.

Keywords: breakout heterogeneities, fracture network, material heterogeneities, weak zones, stress state

1. Introduction

To ensure wellbore stability is one of major problems for drilling in hydrocarbon and geothermal industries, depending on the state of stress and the rock strength [1]. The present day state of stress has a key influence on fluid flow through fractured geo-reservoirs. For example, hydraulically active fractures tend to be critically stressed in the contemporary stress field [2]. Current investigations of stress orientations and magnitudes are based on various methods including analysis of hydraulic fracturing, borehole breakouts [3], drilling induced tensile fractures (DITF), focal mechanism inversion and many others.

Borehole breakouts are cross-sectional elongations in the minimum horizontal stress direction, which are caused by localized failure around a borehole due to stress concentrations [4, 5]. Breakouts are one of the direct indicators of the contemporary tectonic stress field [6]. However, breakout orientations can vary and differ from the mean minimum horizontal stress orientation. We call these localized breakout orientations which differ significantly from the mean minimum horizontal stress “orientation anomalies”. Those orientation anomalies are commonly observed in the vicinity of fracture zones [7].

Paillet and Kim [8] suggested that slip on active faults penetrated by boreholes was the source of breakout anomalies. Barton and Zoback [7], Shamir [9], and Shamir and Zoback [10] compute the local

stress perturbation in the vicinity of fractures, which is required to distort the breakout orientation based on slip on the fault plane. In their studies near complete stress drop on the fracture plane (around 26 MPa at 5400 m depth) is required to match the observed breakout orientation anomalies by this model.

In this paper we consider the changes in mechanical properties affecting the breakout orientation, in particular in the Young's modulus and the Poisson's ratio, induced by the high microcrack density of the fault zone. Fault zones have a high microcrack density near the fault core. This microcrack density decreases exponentially with distance from the fault core[11, 12]. Changes of rock mechanical parameters due to changing crack density could lead to local heterogeneous zones around the fault core [13, 14]. Faulkner et al. [15] showed that crack density influences the elastic properties of rock and, hence, the stress state of surrounding faults. Furthermore, they found that the mean stress as well as the magnitude of the highest principal stress decrease and the least principal stress increase as the fault core is approached, resulting in overall decrease in the differential stress. Thus, the breakout orientation anomalies might also be attributed to varying crack density. Zang et al [16] investigated the petrophysical properties of drill cores of the Continental Deep Drilling Program (KTB) and the relation of foliation, microcrack and stress anisotropy.

Valley [17] analyzed breakouts and drilling-induced tensile fracture (DITF) patterns in two 5 km deep wells of the enhanced geothermal system in Soultz-sous-Forêts (France). He clearly identified a breakout orientation rotation by 50° with a wavelength of about 250 m in the vicinity of a fracture zone supposed to be 400 in m width and length intersecting the well [18]. However, the origin of this deviation remains unclear. He suggests that it might be related to fracture zones that intersect the wells or to lithology changes. In other publications, it is also suggested that such heterogeneity might also be related to minor fracture densities [19], or to fluid pressure [20]. Crack closure pressures have been examined by Zang et al. [21] using ultrasonic P-wave velocities and helped to identify the SH orientation at the KTB site in addition to breakout investigation by Mastin et al [22].

Following the work from Valley [17], details of stress perturbations associated with small natural fractures, not only with major fracture zones, are studied for a better understanding of the impact of the natural fracture network on breakout heterogeneities in granite rock. Herein, we first identify all faults and fractures accompanied by stress-induced breakouts in the crystalline section of the GPK4 well at the Soultz-sous-Forêts geothermal field. Then, we investigate the possible relationship between the breakouts and the mechanical perturbation due to the presence of faults and fractures. We outlined the influence of fracture density to the material heterogeneity, inferred from the detailed analysis of breakout shape. Furthermore, the importance of material heterogeneity resulting from fracture occurrence to breakout development is examined.

2. State of stress in the Soultz-sous-Forêts geothermal field

2.1. Geological context

The Upper Rhine Graben (URG) forms the central part of the European Cenozoic rift system, which consists of a rift-related sedimentary basin bounded by the Rhenish Massif and Vogelsberg volcano in the north and the frontal thrust of Jura Mountains in the south [23]. Major faults in the intra-graben and the shoulder areas, which were derived mainly from 2D seismic interpretation [24], are shown in Figure 1.

The intra-graben faults predominantly strike in N10°E direction parallel to the main border faults, whereas faults in the shoulder areas are bimodal with a main strike orientation towards N45°E and N115°E. These fracture trends are known as the Variscan and Hercynian, respectively. The kinematics of the intra-graben faults is predominantly extensional [25, 26], which suggests that the current maximum principal horizontal stress is oriented parallel to the orientation of those faults (NNE). This is confirmed by the world stress map on a regional scale [6]. Furthermore, it is suggested that the stress regime in the URG varies from normal faulting in the northern part to strike slip faulting in the south [27, 28].

Soultz-sous-Forêts is located in the URG and hosts a deep Enhanced Geothermal System (EGS) test site (Figure 1.a). Its reservoir is in crystalline rocks which are characterized by low matrix porosity. Natural and forced fluid circulation takes place through the fracture network. At its current state of development, the EGS consists of five boreholes, including three deep wells which extend to more than 5000 m depth (Figure 1.b). More information about the Soultz-sous-Forêts EGS can be found in Gerard et al. [29].

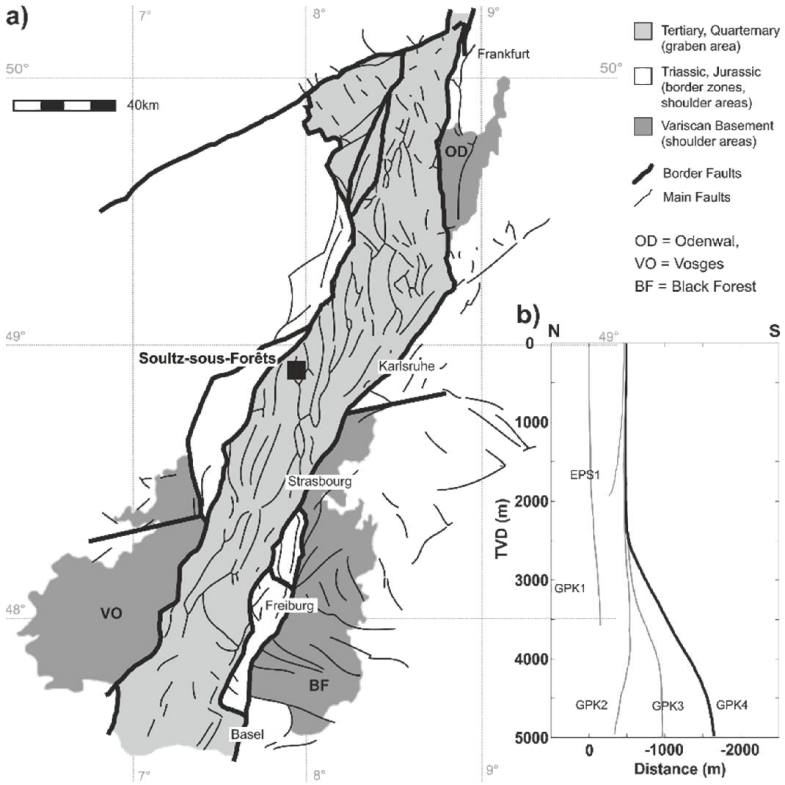

Figure 1: a) Geological map and major fault map of the Upper Rhine Graben rift system modified from Peters (2007). b). N-S cross section of the five wells in the Soultz-sous-Forêts geothermal field.

In-situ stress orientation and magnitude of the Soultz-sous-Forêts geothermal field were inferred from borehole log and hydraulic methods in previous studies. Cornet et al. [30] reviewed various reports and analyses on hydraulic tests, borehole images and induced seismicity. Furthermore, breakouts and drilling-induced tensile fracture (DITF) patterns in GPK3 and GPK4 were analyzed by Valley [17] and Valley and Evans [31]. In general, the mean maximum horizontal stress orientation values fall within the range of N164°E to 185°E.

The natural fracture data of the GPK4 well used in this study were obtained from the French Geological Survey (BRGM) on the GPK4 image logs. Azimuth and dip angle were determined for a total of 1871 fractures along the depth range between 2800 and 5000 m TVD. It can be summarized that most of the fractures appear to be members of a nearly vertical system of a conjugated fracture set with a symmetry axis striking NNW-SSE.

In addition to the BRGM dataset, major fracture zones derived from the geological analysis, induced microseismicity and vertical seismic profiles modeled by Dezayes et al. [32] and Sausse et al. [18] are also incorporated in this analysis. Their notations derived from measured depth are used throughout this study. All fractures and breakouts are presented in TVD (True Vertical Depth), as a result of which the depth of the major fractures plotted in the figure might differ from the depth indicated by their name. Hereinafter, all the natural fractures observed on borehole images and the modeled major structures will be referred to as fractures and fracture zones, respectively.

2.2. Principal horizontal stress orientation inferred from breakout observation

To identify breakouts, we examined the high-quality acoustic borehole televiewer (UBI) log that was run in the granite section of the deep well GPK4. GPK4 is the most deviated well in the Soultz-sous-Forêts geothermal field, its deviation from vertical exceeds 15° in the depth range of 2490–4740 mTVD and reaches a maximum deviation of 35° at 4220 m depth. The UBI tool provides detailed images of the ultrasonic reflectivity of the borehole wall along with the borehole geometry at an angular resolution of 2° inferred from the travel time. The logs were acquired in two runs 15 hours and 18 hours after the completion of drilling, respectively. Hence, the effect of time-dependent breakout growth [33] was probably still insignificant.

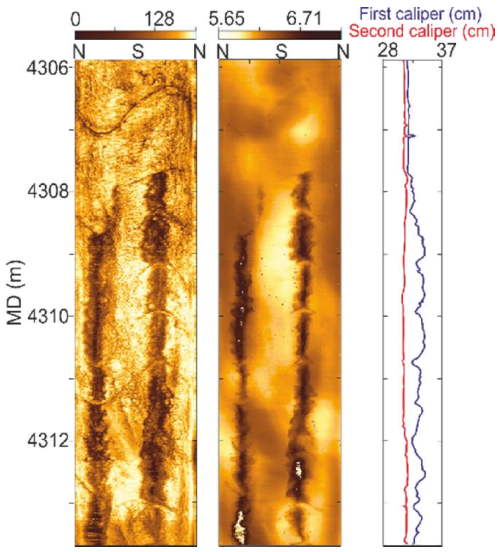

Figure 2: Typical breakout observed in UBI images. Breakouts appear as pair of broad zones of low amplitude (dark zones) on the amplitude log (left) and increased borehole radius (dark zones) on opposite sides of the borehole on the travel time log (mid). Caliper data were also used to measure the depth of the borehole elongation (right).

On the UBI image, breakouts appear as broad zones of increased borehole radius on the travel time log and low amplitude on opposite sides of the borehole on the amplitude log. Typical breakouts observed on the UBI image are shown in Figure 2. Median filtering with a kernel half width of 7 samples (corresponding to 14°) was applied to remove noise in the image data through a one-dimensional linear filter. Stress-induced borehole elongations are not always observed symmetrically in opposite directions. In some cases, they might be confused with key seat or washout phenomena [34]. Elongation pairs separated by at least 130° with an increase of the borehole radius of more than 2% were picked as breakouts.

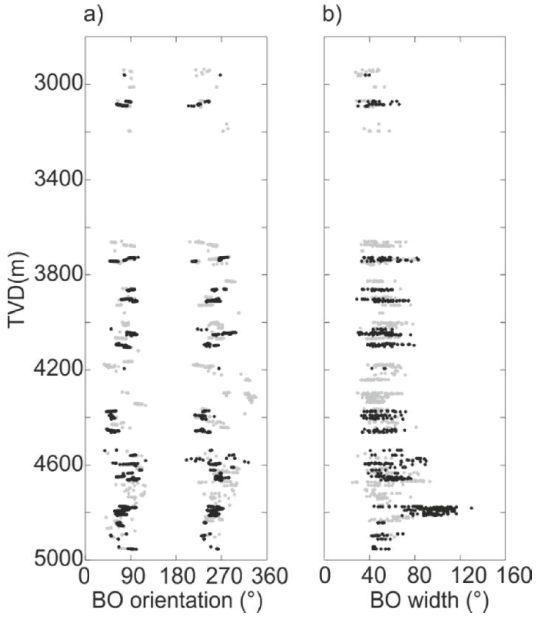

Figure 3: Stress-induced borehole elongation observations from the GPK4 UBI log. a) Breakout orientations. b) Breakout widths. Black and gray circles denote high and and low confidence intervals, respectively.

Figure 3 shows an overview of the borehole breakout observation as discussed subsequently. Breakouts were observed starting at a depth of 2900 mTVD. The orientation and width of borehole elongation trends seen on UBI images were then measured every 20 cm. Both sides of the breakouts

were picked. A total of 1221 borehole elongation pairs were identified. Each elongation pair is then considered an individual breakout with a uniform length of 20 cm. This approach enabled us to examine the detailed breakout shape on both sides and its correlation with the occurrence of fractures.

Two breakout data qualities were distinguished. Good breakouts picked from good quality image data are drawn in black. On average, they have picking uncertainty of 5° and 8° in orientation and width, respectively. Gray dots indicate lower quality that is mainly due to logging artefacts or intersections with a dense fracture zone, which made the selection of the breakouts more difficult. Consequently, they have a higher uncertainty of 8° and 10° for orientation and width, respectively (Figure 3). The high quality breakouts are then given double weights for the following analyses.

Most breakout widths are less than 110°, with 90% of the values lying in the range of 38°–97°, although wider breakouts were observed in some depth intervals (Figure 3.b). The breakouts reveal that the average orientation of the minimum horizontal stress (ASh) is N78° ± 17°E. This result is in agreement with the results obtained in previous studies [17, 30].

2.3. Detailed breakout shape analysis and its correlation with fracture densities

Obviously, stress-induced borehole elongations are not distributed homogeneously along the depth, e.g. no breakouts were observed in the interval 3400-3600 mTVD depth and substantially higher numbers of breakouts were observed in the sections several hundred meters above and below. Additionally, breakouts were also observed to be asymmetrically formed. A detailed analysis of the breakout shape was conducted to gain more insight into material heterogeneities in the vicinity of the borehole. It was supposed that the intersection between fractures and the borehole might create damaged zones at the borehole wall which modify the geo-mechanical properties. Especially the Young's modulus of such damaged zones should decrease when approaching the fracture core and the breakout elongation might rather develop towards the damaged weak zones. Hence, the final breakout might be perturbed from its ideal symmetrical shape as proposed for a homogeneous isotropic material (Figure 4).

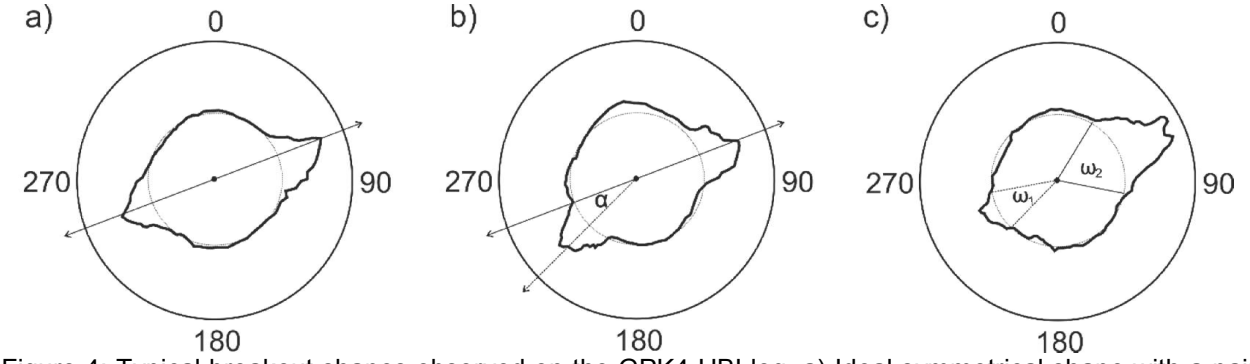

Figure 4: Typical breakout shapes observed on the GPK4 UBI log. a) Ideal symmetrical shape with a pair of identical elongations in opposite directions. b) One elongation side is shifted by α from its ideal orientation. c) The elongations concentrated on one side only. As a result, one side has a wider and deeper elongation than the other.

To investigate this assumption, the orientation deviations α and width differences $\Delta\omega = |\omega_1 - \omega_2|$ (Figure 4) were calculated for each breakout pair. Mean filtering with a moving window of 5 m was applied to smooth the profiles. Breakouts which have low orientation deviation α tend to have low width difference $\Delta\omega$, and vice versa. The orientation and width differences are found to be up to 37° and 18°, respectively (Figure 5.c and d).

The intersection of the fracture with the borehole will create a weak zone which might be a preferred location for breakout to develop. The upper and lower intersections of the fracture with the well, however, are separated by a distance depending on the fracture inclination. Here, a single fracture might only affect one side of the breakout at a particular depth. This effect will be amplified in a high fracture density zone, hence the most dense and asymmetric breakouts are observed in the high fracture density zone.

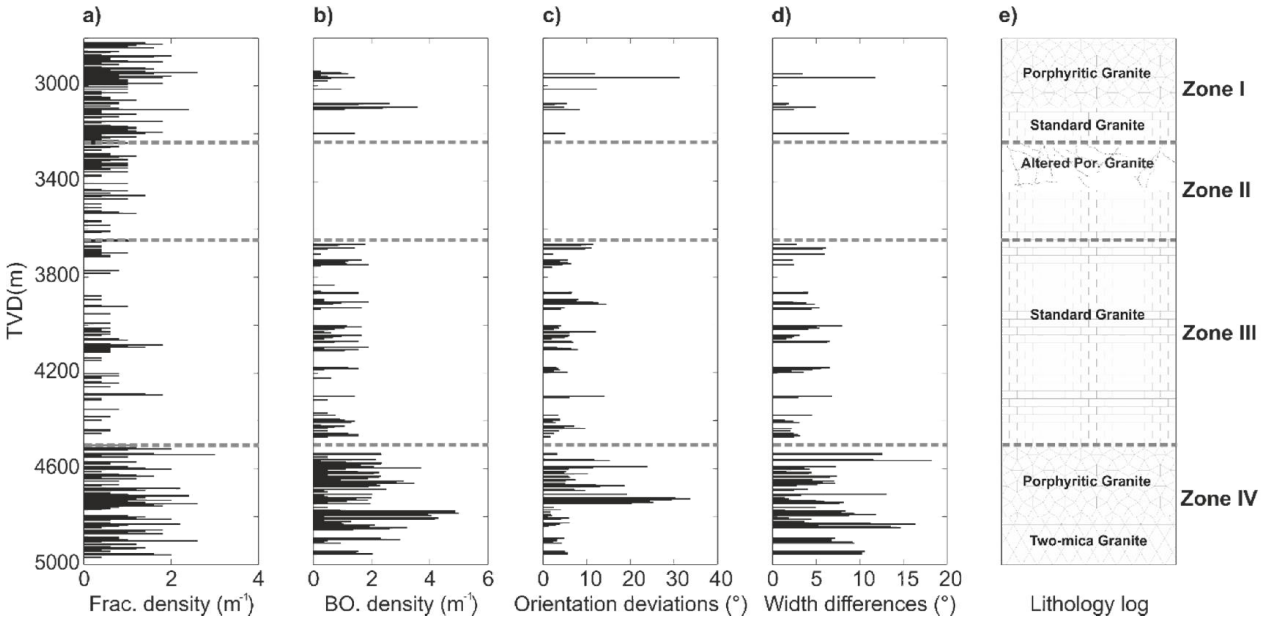

Figure 5: Results of the detailed breakout shape analysis and its correlation with lithology and the occurrence of fracture intersecting borehole. a) Fracture density. b) Breakout density. c) Breakout orientation deviations from its ideal opposite direction. d) Width differences of the pair elongation. e) Lithology log. Four zones were distinguished based on the occurrence of breakouts and their detailed shape and with comparison of fracture occurrence.

A crossplot of breakout density and fracture density (Figure 6) shows a clustering of breakout-fracture pairs consistent with four depth zones. These zones are consistent also with breakout asymmetry (Figure 5) and the petrographic model of the Soultz-sous-Forêts geothermal field by Hooijkaas et al. [34]. In a simplified manner, four different zones of breakout and fracture occurrence can be distinguished:

Zone I: This uppermost zone from 2900 to 3200 mTVD has a high fracture density of about 0.48 to 1.8 m^{-1}, but the breakout density is low. This zone consists of massive porphyritic granite which is highly fractured and hydrothermally altered.

Zone II: Zone without breakouts between 3200 and 3600 mTVD. No further analysis was conducted for this section. This zone is characterized by a rather low fracture density and dominated by altered porphyritic granite section. In this altered granite section the borehole image quality is very poor and did not allow for breakout analysis.

Zone III: The middle zone between 3600 and 4500 mTVD is characterized by small fracture densities and breakout occurrences. Breakout pair orientation deviation and width difference also are quite small in this zone. In this depth interval, the granite is less fractured and is very rich in biotite and amphibole.

Zone IV: The lowermost part zone from 4500 to 5000 mTVD is characterized by a high density of both fractures and breakouts, up to 2.3 m^{-1} and breakouts were observed continuously over several tens of meters. A younger, fine-grained, two-mica and amphibole-rich granite that intrudes into the porphyritic granites is predominating in this zone.

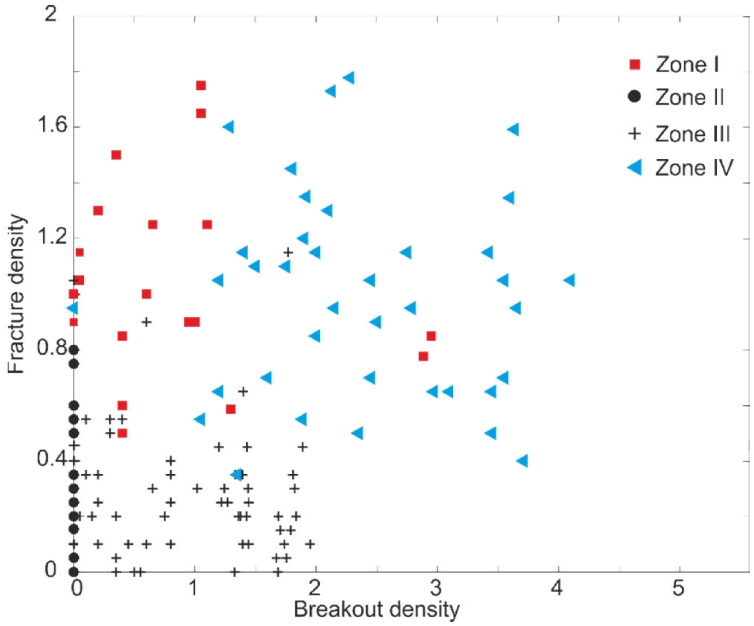

Figure 6: Crossplot between fracture density and breakout density observed in the crystalline section of the GPK4 well.

3. Breakout heterogeneity and its connection with fracture networks

The origin of the breakout orientation heterogeneities shall be analyzed in the present section. Mastin [35] found that breakout orientation is rotated away from the direction of the minimum horizontal stress, as the borehole deviates from the direction of the sub-vertical principal stress. He calculated the minimum value of borehole deviation (critical angle) for all borehole azimuths to rotate the breakout orientation by 10°. Considering the stress magnitude analyses of Valley [17] and Cornet et al. [30] who find the stress regime to be a transitional strike slip to normal faulting, the critical deviation angle for a breakout rotation by more than 10° is around 35°, which corresponds to the maximum deviation of GPK4 well. Hence, breakouts might be rotated by a maximum of 10° from ASh due to well inclination. The rotations observed in GPK4 well, however, showed much higher values. Consequently, it can be concluded that this is not the sole effect of borehole deviation.

Systematic or abrupt breakout orientation rotations were frequently observed in the intersection zone of fractures with the GPK4 borehole wall. Furthermore, shapes of breakouts were found to be the most asymmetric in the zone of the highest fracture density (below 4500 mTVD). When assuming the reservoir to be composed of homogeneous granite, it is reasonable to assume that the source of breakout heterogeneities is the occurrence of weak zones in the vicinity of fractures.

By analyzing the perturbation of breakout orientations in the vicinity of fracture, two main questions regarding the role of fractures shall be answered: Are there patterns of breakout orientation in the vicinity of fractures? What is the main factor that controls the breakout orientation rotation? Breakout analyses are performed in the vicinity of both fracture zones and fractures.

3.1 Influence of fracture zones

It was observed in several fields that the principal horizontal stress orientations varies with depth [7, 8]. In the following, we investigate the large-scale breakout orientation rotation trend with depth and its correlation with fracture zones. The whole survey depth range was divided into 10 sub-ranges according to the occurrence or lack of breakouts, their orientation variations, and also considering the intersection with fracture zones. All fracture zones used in this analysis have length and width of more than 300 m [18]

Figure 7 shows the one-sided breakout plot of the breakout orientation with depth. This is the averaged orientation of both borehole elongations in each pair shown in Figure 3.a, plotted in N0°-180°E half-circle. The azimuthal deviations represented in each box plot can be considered as including measurement errors, local heterogeneities and variations of the stress orientation.

The median orientations of the breakout groups above 4150 mTVD are consistent with the ASh orientation. In this depth range, only a low to medium density of fracture ($0.43m^{-1}$) and one fracture zone

are observed. A long section of absence of breakouts is observed between 3230 and 3600 mTVD. DITF are also absent in this depth interval [17]. Below this section, the FZ-3940 fracture zone is found at 3770 mTVD. Although the median orientation of breakouts is consistent with ASh, breakouts are found to be heterogeneously oriented in the vicinity of the fracture zone. The 1st and 3rd quartiles of the breakout orientations are N60°E and N100°E, respectively. Damage area surrounding the fracture core might be the source of these large heterogeneities of breakout orientation.

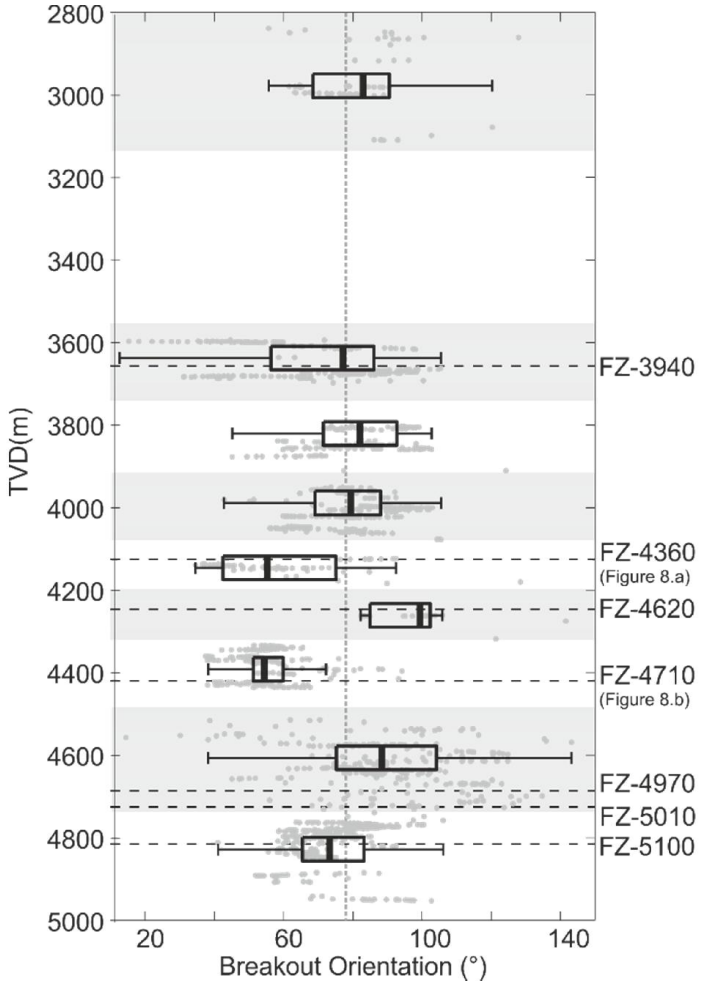

Figure 7: Profile of breakout orientations in the GPK4 well. Box plots are used to summarize the distribution of depth intervals. The lower and upper fences, the 1st and 3rd quartiles (rectangle) as well as the median value are plotted. The depths of the intersected major fractures are indicated by dashed lines.

In the vicinity of the fracture zone FZ-4360, most of the observed breakout orientations are rotated from ASh in counterclockwise direction. The median is found to be deviated by 13° (Figure 7). A closer look at the breakouts orientation in the vicinity of FZ-4360 is shown in Figure 8.a. The distribution of the breakout orientation above the fracture (from 4090 mTVD) and below it (up to 4185 mTVD) follows a sinusoidal curve with its highest shift at depth of the fracture core. Above the fracture, the breakout orientations increase from -27 to 22° relative to ASh; and below the orientations decrease to -40°. Overall an orientation variation of about 60° is observed. However, breakouts were absent in the vicinity of FZ-4360 fracture core. Such a breakout absent zone was also observed in several other fields, e.g. [7, 36]. The role of the FZ-4360 fracture zone seems to prevent breakout formation in its vicinity. This suggests that the magnitude of the differential stresses is reduced in the immediate vicinity of FZ-4360. Possible mechanisms are plasticity or creep [37].

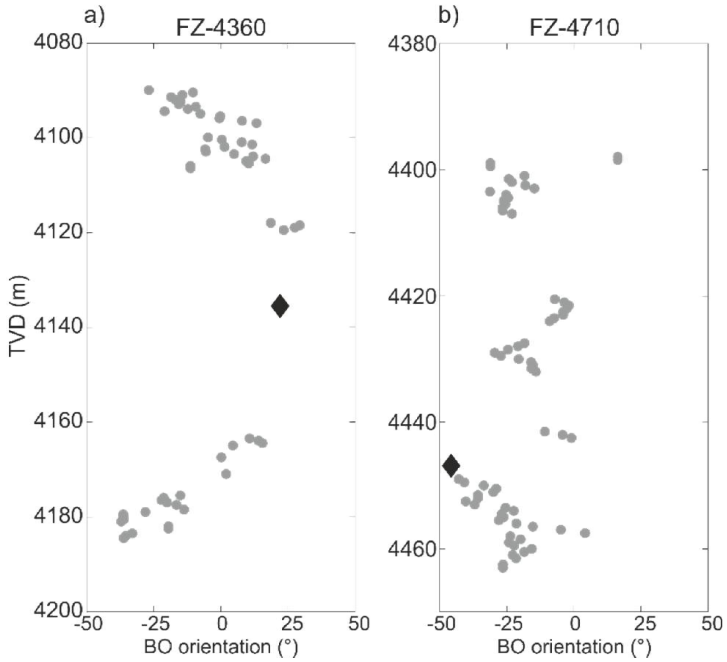

Figure 8: Breakout orientation profile with depth around three fracture zones: a) FZ-4360, and b) FZ-4710. Gray dots indicate borehole breakout orientations, black diamond display the fracture zones dip direction. All orientations are plotted relative to ASh.

Only few breakouts are observed in the vicinity of FZ-4620. All those breakouts are oriented toward clockwise direction from ASh (Figure 7). FZ-4710 is found around 80 m below FZ-4620. This fracture zone is a Hercynian fracture and intersecting the GPK4 well with the lowest inclination [23, 38]. Numerous breakouts were observed in its vicinity, and almost all of them (96%) are shifted counterclockwise from ASh. Interestingly, FZ-4710 is also dipping toward counterclockwise direction relative to ASh. The parallel orientation of both major fracture dip azimuth and breakout orientation was also observed for FZ-4620. Breakout patterns in the vicinity of both major fracture zones suggest that breakout orientation, in a low to moderate fracture density zone, were rotated from ASh to a preferred direction which might be controlled by its dip azimuth.

A closer look at the breakout patterns in the vicinity of FZ-4710 is shown in Figure 8.b. Around the fracture zone, breakouts have the highest orientation rotation at the fault core. Breakout orientation trends were dominated by negative shifts. It is obvious that the fault initiated the breakout, starting from the borehole elongation towards the azimuth of the fault dip (clockwise 46° deviation) and gradually returns to ASh with increasing distance from the fault core. The two distinct breakout patterns in the vicinity of FZ-4360 and FZ-4710 fracture zones suggest the role of fracture zones in breakout heterogeneity, either in preventing breakout occurrence or rotating their orientation.

Three fracture zones and a large number of fractures are observed in the deepest two sub-ranges. Hence, it is not surprising that the most heterogeneous breakout orientation zones are found in this part. Additionally, it is also shown that an enhanced presence of fractures correlates well with an enhanced occurrence of breakouts. For example the depth interval of 4700 – 4830 mTVD has the highest density of fractures intersecting the well and also the most densely observed breakouts.

3.2 Influences of natural fractures

A detailed observation of the breakout orientation in the vicinity minor fractures was performed to gain a better understanding of the relationship between breakouts and fracture orientation. Breakouts were found in the vicinity of 25% of fractures found in GPK4. Only those fractures accompanied by stress-induced borehole breakouts were selected for further analysis.

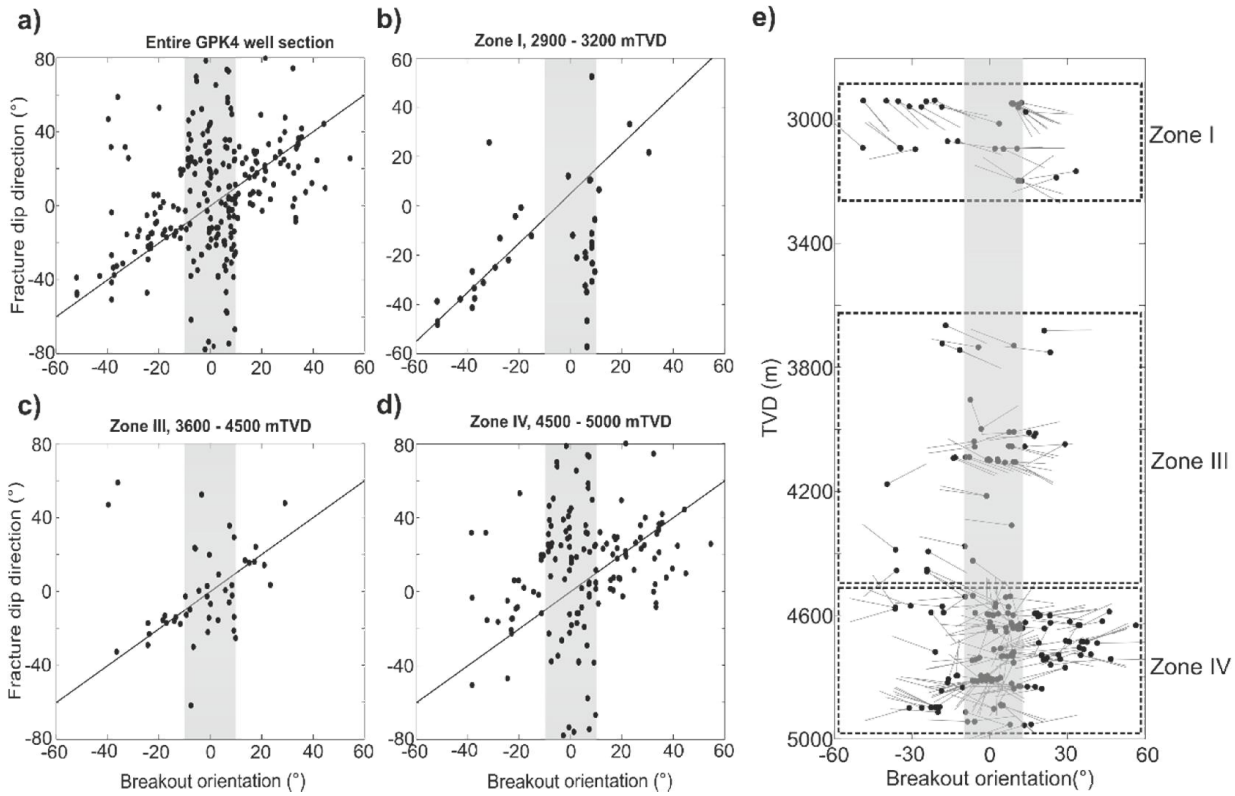

Figure 9: Cross-plot between fracture dip directions and averaged breakout orientations observed in the vicinities of fractures in (a) the entire GPK4 well, (b) zone I, (c) zone III and (d) zone IV. The gray area indicates the unperturbed breakouts orientation. (e) Tadpoles of breakout orientation to the fracture direction of each breakout-fracture pair versus TVD. Zero for all orientation axes is the ASh.

Cross-plots of fracture dip direction and average breakout orientation observed 3 m around each fracture was made (Figure 9). Both breakout and fracture orientations are plotted relative to ASh. The orientation deviations of both parameters are expressed in either clockwise (positive) or counterclockwise (negative) deviation. The purpose was to determine the deviation of breakout orientation and its correlation with the orientation of the fractures intersecting the borehole.

The correlation coefficient was calculated to measure the statistical relationship between those sets of orientation data. As the coefficient approaches zero, there is no correlation between fracture and breakout orientation. The closer it is to either −1 or 1, the stronger is the correlation between the variables.

Figure 9.a shows the cross-plot for the entire GPK4 well. Several breakout-fracture pairs are oriented towards ASh orientation. These breakout-fracture pairs fall in the gray area. The orientation of those breakouts is consistent with the ASh orientation. This indicates that the stress state remains mostly constant around those fractures.

However, breakout orientations in the vicinity of many other fractures are found to be rotated from ASh by up to 60°. Hence, two breakout orientation trends in the vicinity of natural fractures can be distinguished in this plot. First, breakouts oriented about ASh and second, breakouts oriented more than 10° off from ASh. Only those fractures accompanied by breakouts deviated by more than 10° from ASh are used in this analysis.. The threshold of 10° was used to consider the effect of borehole deviation on the breakout orientation and breakout picking uncertainties.

The black diagonal in the crossplots indicates a breakout orientation parallel to the fracture dip direction. In general, those breakout- fracture pairs are found very close to this trend, with a standard deviation of the azimuth of 17°. The correlation coefficient between both orientations is 0.6. This value indicates that there is distinct correlation between the breakout orientation rotation and the fracture orientation.

More detailed analysis of breakout-fracture pairs is conducted for the four different zones described in chapter 2.3 to analyze the correlation in each zone. The correlation between fractures and breakout

orientations is very pronounced in the first zone (Figure 9.b). Here, breakout orientation rotations are dominated by counterclockwise deviation from ASh with a maximum shift of 48°. The pairs of breakouts and fractures are scattered along the black diagonal, indicating a direct relation, with a standard deviation of only 7°. This strong correlation is also reflected by a high correlation coefficient of 0.90. Interestingly, only one fracture family is present in this section, with all fractures dipping in similar directions.

A good correlation coefficient of 0.83 was obtained in the third zone (Figure 9.c). Around 50% of the fractures accompanied by breakouts in this zone were related to their surrounding breakout orientation deviation. Clockwise and counterclockwise deviations of up to 40° and 30°, respectively, were observed.

Such a strong connection was not observed in the fourth zone (Figure 9.d). Here, only a low correlation coefficient of 0.32 was obtained for breakout orientation in the vicinity of fractures. This is probably due to the high density of fractures observed in this zone. As observed in the previous studies, [6, 36], the breakout azimuths varies significantly on length scales of few centimeters to hundreds of meters as a function of depth along the well bore. Given the averaged distance between the fractures in this zone (3.9 m), it is reasonable to assume that the perturbation effect of one fracture might overlap with that of the neighboring fractures. Therefore no good correlation was observed in this zone.

Although the upper zone also has a high fracture density, the overlapping effect seems not to be dominant. This suggests that the overlapping effect is not only due to the high density of fractures. As the breakout orientation perturbation is affected strongly by the fracture orientation, it is reasonable to assume that it might be also due to the fracture network orientation. The upper zone has fractures which are uniformly dipping counterclockwise relative to ASh (Figure 9.e). In such a case, the overlapping effect still occurs, but breakouts are rotated consistently toward the same direction. Hence a good correlation can be achieved. The lower zone is not only highly fractured but the fractures are also heterogeneously oriented. As a result, the breakout-fracture orientation plot exhibits scattering with a very weak correlation. This shows the importance of fracture density and of their orientation on breakout orientation perturbations.

4. Discussions

The effect of fractures on the mechanical properties of rock was analyzed in many studies. In-situ laboratory measurements on Soultz-sous-Forêts granite [17] revealed the effect of fractures on rock mechanical parameters. Young's modulus of intact Soultz-sous-Forêts granite was determined to be around 54 GPa, but only 39 GPa for significantly fractured granite. Furthermore, the uniaxial compressive strength is also found to decrease with increasing fracture density [39]. Due to the reduction of rock strength, breakout is expected to develop more easily. Hence, a good correlation between the density of fractures intersecting the well and observed breakouts could be expected.

If a fault zone has an associated fractures damaged zone, the stresses are expected to be perturbed and rotated depending on the change in elastic properties of the damaged material. As the fault core bears the most damage, the stress perturbation is assumed to be concentrated in that zone and to decrease with distance. Breakouts will then develop according to this local stress perturbation. In such a case, a gradual breakout orientation rotation centered at the fault core is expected to result. This gradual rotation trend starting from the fault core is observed well in the vicinity of GPK4-FZ4620 (Figure 8.b).

The dimensions of natural fractures are too small to induce local stress perturbations required to alter the breakouts orientation [7]. Hence, we attribute the observed small wavelength breakout rotation in the vicinity of a natural fracture to the material heterogeneity due to the occurrence of weak zones in the vicinity of fractures. A conceptual model, supported by the strong correlation between breakout and fracture orientations in the first and second zones of the well, of the perturbed breakout shape in a heterogeneous material is shown in Figure 10. The weak zone is assumed to be the result of the increasing microcrack density in the fracture core. This typically reduces the stiffness (Young's modulus) and increases Poisson's ratio [14].Furthermore, it has been shown that changes in elastic moduli can induce changes in the stress field [13]. Haimson [40] showed that in an intact granite the breakout is initiated by the development of the microcracks subparallel to the maximum horizontal stress direction behind the borehole wall. In a heterogeneous material, such microcracks are already present in the weak zone. Hence, the perturbed breakout shape is then developing along this weak zone.

The different role of fractures in affecting breakout orientation was shown. Some fractures induce a breakout orientation rotation in their vicinity, while others do not. An attempt was made to distinguish those two different type of fractures based on their orientation and dip angle. Fractures that perturbed breakout orientation in its vicinity have dip direction from N105°NE to N219°E and dip angles between 30° and 88°,

which covers almost the entire range of all fractures observed in this well. Hence, no clear separation could be obtained.

Fractures that perturb the orientation of breakouts might have experienced slippage prior to drilling [7], or different lithologies [36]. Another possibility is that those fractures significantly alters the mechanical material properties in the vicinity [13, 15]. The latter is more probable, as laboratory measurements [17] also showed that the reduction of the rock strength due to fractures depends on its fracture filling mineral. Fractures with quartz sealing may be almost as strong as the intact rock, while sulfide sealed fractures show a rock strength reduction by almost 50%.

We also observe the importance of fracture inclination on breakout development. For nearly vertical fracture dipping, the top and bottom intersections of a single fracture with a borehole of 12.25 inch in diameter might be separated by a couple of meters. Here, fracture might only affect one side of the breakout at a particular depth. As a result asymmetrical shapes of breakouts will be expected. Furthermore, the overlapping effect of adjacent fractures might increase material heterogeneities, as the most asymmetric breakout shapes are observed in the high fracture density zone.

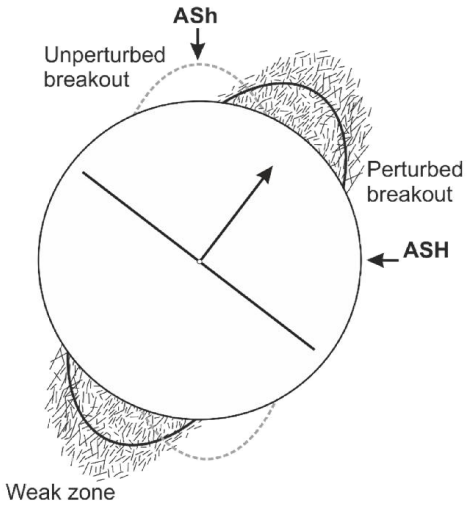

Figure 10: Sketch of the perturbed breakout shape in a heterogeneous material. The breakouts are rotated from the unperturbed breakouts (black elongations) toward the weak zone, i.e. weak zones are assumed to be the results of the intersection between natural fracture and borehole wall.

5. Conclusions

Analyzing detailed breakout heterogeneities and their correlation with fracture occurrence at great depth is a challenging task, in particular because of lacking information on in-situ material properties of fractured rock. While our determined mean direction of S_{hmin} agrees well with previous studies [17, 30], careful analysis shows that breakout orientations are systematically affected by the occurrence of fractures and fracture zones. We propose two different mechanisms for the breakout rotation in the vicinity of fracture zones and natural fractures. For breakouts around fracture zones, examples of systematic sinusoidal perturbations to breakout orientation, initiation and inhibition of breakout formation were presented. Therefore we conclude, that anomalies of breakout orientation in the vicinity of fracture zones reflect the large-scale stress heterogeneity caused by the fracture zones.

The analyzed well section was divided into four distinct sections, based on the correlation of breakout and natural fracture densities. It was shown that breakout occurrence, orientation, and shape symmetry are largely determined by the fracture network. Crossplots of breakout orientation and fracture dip direction reveal a direct correlation of both features. This correlation is highest for sections with only one fracture family present and is less in heterogeneous zones with high fracture density and several fracture families (Figure 9). Since Barton and Zoback [7] found that natural fractures are too small to perturb the stress field even locally, the observed perturbations of breakout orientation cannot be explained by a perturbation of the stress field. However, the direct relation of fracture dip direction and breakout orientation suggests that weak zones surrounding the fractures are causing the breakouts to form along the fracture dip directions. If slippage would perturb the stress field, no consistent correlation with fracture

dip direction would be expected, since the slip direction would change according to the direction of maximum shear stress [41].

In the Fourth Zone, with a high fracture density the overlapping effects of several fracture families present reduces the correlation of fracture dip direction and breakout orientation. In this section we also observe the largest asymmetries, evidenced by different widths of opposite breakouts and also a distance between an elongation pair smaller than 180° along the borehole wall. We conclude that asymmetric breakouts are caused by the weak zones accompanying steeply dipping fractures, which are penetrated by the borehole over a length of up to several meters.

The results of this study provide a better understanding of stress-induced borehole elongations in fractured rocks. Careful analysis of breakouts can help us learn about the mechanical properties of fractures and their immediate surroundings. The impact of the fracture network on breakout heterogeneities is very pronounced in crystalline rock, which is mechanically isotropic. This is why we could attribute the perturbation of breakouts to the occurrence of fractures and accompanying alteration of mechanical properties only. Numerical modeling taking into account the elastic property changes as a result of fracturing and fracture filling is required to better quantify the phenomena observed in this study.

6. Acknowledgements

The authors are grateful to the DIKTI and DAAD for the financial support of the research, to the BRGM for providing the Soultz natural fractures data, and to the GEIE EMC for providing the geophysical log data from the Soultz wells.

References

[1] Moos D, Peska P, Finkbeiner T, Zoback MD. Comprehensive wellbore stability analysis utilizing quantitative risk assesment. Journal of Petroleum Science and Engineering. 2003;38:97-109.

[2] Barton CA, Zoback MD, Moos D. Fluid flow along potentially active faults in crystalline rock. Geology. 1995;23.

[3] Bell JS, Gough DI. Northeast-southwest compressive stress in Alberta: evidence from oil wells. Earth and planetary science letters. 1979;45:475-82.

[4] Zheng Z, Kemeny K, Cook NGW. Analysis of borehole breakouts. Journal of Geophysical Research. 1989;94:7171-82.

[5] Zoback MD, Moos D, Mastin L, Anderson RN. Wellbore breakouts and in situ stress. Journal of Geophysical Research. 1985;90:5523-30.

[6] Heidbach O, Tingay M, Barth A, Reinecker J, Kurfeß D, Müller B. The world stress map database release 2008 doi:10.1594/GFZ.WSM.Rel2008. 2008.

[7] Barton CA, Zoback MD. Stress perturbations associated with active faults penetrated by boreholes: Possible evidence for near-complete stress drop and a new technique for stress magnitude measurement. Journal of Geophysical Research. 1994;99:9373-90.

[8] Paillet FL, Kim K. Character and Distribution of Borehole Breakouts and Their Relationship to in Situ Stresses in Deep Columbia River Basalts. Journal of Geophysical Research. 1987;92:6223-34.

[9] Shamir G. Crustal stress orientation profile to a depth of 3.5km near the San Andreas fault at Cajon Pass, California. Stanford: Stanford University; 1990.

[10] Shamir G, Zoback MD. Stress orientation profile to 3.5 km depth near the San Andreas Fault at Cajon Pass, California. Journal of Geophysical Research. 1992;97:5059-80.

[11] Janssen C, Wagner FC, Zang A, Dresen G. Fracture process zone in granite: a microstructural analysis. International Journal Earth Sciences (Geol Rundsch). 2001;90:46-59.

[12] Vermilye JM, Scholz CH. The process zone: A microstructural view of fault growth. Journal of Geophysical Research. 1998;103:12223-37.

[13] Heap MJ, Faulkner DR. Quantifying the evolution of static elastic properties as crystalline rock approaches failure. International Journal of Rock Mechanics and Mining Sciences. 2008;45:564-73.

[14] Heap MJ, Faulkner DR, Meredith PG, Vinciguerra S. Elastic moduli evolution and accompanying stress changes with increasing crack damage: implication for stress change around fault zones and volcanoes during deformation Geophysical Journal International. 2010;183:225-36.

[15] Faulkner DR, Mitchell TM, Healy D, Heap MJ. Slip on 'weak' faults by the rotation of regional stress in the fracture damage zone. Nature. 2006;444:922-5.

[16] Zang A, Wolter K, Berckhemer H. Strain recovery, microcracks and elastic anisotropy of drill cores from KTB deep well. Scientific drilling: geophysics, geochemistry and technology. 1989;1:115-26.
[17] Valley BC. The relation between natural fracturing and stress heterogeneities in deep-seated crystalline rocks at Soultz-sous-Forets (France). Zurich: Swiss Federal Institute of Technology Zurich; 2007.
[18] Sausse J, Dezayes C, Dorbath L, Genter A, Place J. 3D model of fracture zones at Soultz-sous-Forets based on geological data, image logs, induced microseismicity and vertical profiles. Comptes Rendus Geoscience. 2010;342:531-45.
[19] Sikaneta S, Evans KF. Stress heterogeneity and natural fractures in the Basel EGS granite reservoir inferred from an acoustic televiewer inferred from an acoustic televiewer log of the Basel-1 Well. Thirty-seventh workshop on geothermal reservoir engineering. Stanford2012. p. SGP-TR-194.
[20] Chang C, Haimson B. Effect of fluid pressure on rock compressive failure in a nearly impermeable crystalline rock: Implication on mechanism of borehole breakouts. Engineering Geology. 2006;89:230-42.
[21] Zang A, Berckhemer H, Lienert M. Crack closure pressures inferred from ultrasonic drill-core measurements to 8 km depth in the KTB wells. Geophysical Journal International. 1996;124:657-74.
[22] Mastin L, Heinemann B, Krammer A, Fuchs K, Zoback MD. Stress orientation in the KTB pilot hole determined from wellbore breakouts. Scientific drilling: geophysics, geochemistry and technology. 1991;2:1-12.
[23] Ziegler PA. Cenozoic rift system of western and central Europe: an overview. Geologie en Mijnbouw. 1994;73:99-127.
[24] Peters G. Active tectonics in the Upper Rhine Graben: Integration of Paleoseismology, Geomorphology and Geomechanical modeling. Amsterdam: University Amsterdam; 2007.
[25] Cardozo GL, Behrmann JH. Kinematic analysis of the Upper Rhine Graben boundary fault system. Journal of Structural Geology. 2006;28:1028-39.
[26] Ford M, Veslud CLC, Bourgeois O. Kinematic and geometric analysis of fault-related folds in a rift setting: The Dannemarie basin, Upper Rhine Graben, France. Journal of Structural Geology. 2007;29.
[27] Larroque JM, Etchecopar A, Philip H. Evidence for the permutation of stresses σ_1 and σ_2 in the Alpine foreland: the example of the Rhine graben. Tectonophysics. 1987;144:315-22.
[28] Rotstein Y, Schaming M. The Upper Rhine Graben (URG) revisited: Miocene transtension and transpression account for the observed first-order structures. Tectonics. 2011;30:TC3007.
[29] Gerard A, Genter A, Kohl T, Lutz P, Rose P, Rummel F. The deep EGS (Enhanced Geothermal System) project at Soultz-sous-Forêts (Alsace, France). Geothermics. 2006;35:473-83.
[30] Cornet FH, Berard T, Bourouis S. How close to failure is a granite rock mass at a 5 km depth? International Journal of Rock Mechanics and Mining Sciences. 2007;44:47-66.
[31] Valley BC, Evans KF. Stress state at Soultz-sous-Foretz to 5 km depth from wellbore failure and hydraulic observations. Thirty-Second Workshop on Geothermal Reservoir Engineering. Stanford, US2007. p. SGP-TR-183.
[32] Dezayes C, Genter A, Valley BC. Structure of the low permeable naturally fractured geothermal reservoir at Soultz. Comptes Rendus Geoscience. 2010;342:517-30.
[33] Schoenball M, Sahara D, Kohl T. Time-dependent brittle creep as mechanism for time-delayed wellbore failure. International Journal of Rock Mechanics and Mining Sciences, 70, 400-406. 2014.
[34] Plumb RA, Hickman SH. Stress-induced borehole elongation: A comparison between the four-arm dipmeter and the borehole televiewer in the Auburn Geothermal Well. Journal of Geophysical Research. 1985;90:5513-21.
[35] Mastin L. Effect of Borehole Deviation on Breakout Orientations. Journal of Geophysical Research. 1988;93:9187-95.
[36] Lin W, Yeh E-H, Hung J-H, Haimson B, Hirono T. Localized rotation of principal stress around faults and fractures determined from borehole breakouts in hole B of the Taiwan Chelungpu-fault Drilling Project (TCDP). Tectonophysics. 2010;482:82-91.
[37] Sibson RH. Fault rocks and fault mechanisms. Journal of the Geological Society 1977;133:191-213.
[38] Hurd O, Zoback MD. Intraplate earthquakes, regional stress and fault mechanics in the Central and Eastern U.S. and Southeastern Canada. Tectonophysics. 2012;581:182-92.
[39] Alm O, Jaktlund L-L, Shaoquan K. The influence of microcrack density on the elastic and fracture mechanical properties of Stripa granite. Physics of the Earth and Planetary Interiors. 1985;40:161-79.
[40] Haimson B. Micromechanisms of borehole instability leading to breakouts in rocks. International Journal of Rock Mechanics and Mining Sciences. 2007;44:157-73.
[41] Bott MHP. The mechanics of oblique slip faulting. Geological Magazine. 1959;96:109-17.